The impact of allometry on vomer shape and its implications for the taxonomy and cranial kinesis of crown-group birds

Olivia Plateau[1]*, Christian Foth[1]

[1]Department of Geosciences, University of Fribourg, Chemin du Musée 6, CH-1700 Fribourg, Switzerland

*e-mail: olivia.plateau@unifr.ch

O.P. (ORCID: 0000-0002-8321-2687)

C.F. (ORCID: 0000-0002-9410-4569)

Abstract

Crown birds are subdivided into two main groups, Palaeognathae and Neognathae, that can be distinguished, among others, by the organization of the bones in their pterygoid-palatine complex (PPC). Shape variation to the vomer, which is the most anterior part of the PPC, was recently analysed by Hu et al. (2019) with help of geometric morphometrics to discover morphological differences between palaeognath and neognath birds. Based on this study, the vomer was identified as sufficient to distinguish the two main groups (and even more inclusive neognath groups) and their cranial kinetic system. As there are notable size differences between the skulls of palaeognaths and neognaths, we here investigate the impact of allometry on vomeral shape and its implication for taxonomic classification by re-analysing the data of the previous study. Different types of multivariate statistical analyses reveal that taxonomic identification based on vomeral shape is strongly impaired by allometry, as the error of correct identification is high when shape data is corrected for size. This finding is evident by a great overlap between palaeognath and neognath subclades in

morphospace. The correct identification is further influenced by the convergent presence of a flattened vomeral morphotype in multiple neognath subclades. As the evolution of cranial kinesis has been linked to vomeral shape in the original study, the existing correlation between shape and size of the vomer across different bird groups found in the present study questions this conclusion. In fact, cranial kinesis in crown birds results from the loss of the jugal-postorbital bar in the temporal region and ectopterygoid in the PPC and the combination of a mobilized quadrate-zygomatic arch complex and a flexible PPC. Therefore, we can conclude that the vomer itself is not a suitable proxy for exploring the evolution of cranial kinesis in crown birds and their ancestors.

Introduction

The pterygoid-palatine complex (PPC) of crown birds is mainly formed by five bones: the unpaired vomer that results from the fusion of the originally paired vomer elements and the paired pterygoids and palatines. Its general morphology was first studied by Huxley (1867), who distinguished the clade Palaeognathae from all other birds on the basis of palatal morphology. Although the PPC of palaeognaths is quite variable (McDowell 1948), it is characterized by a large vomer that is only partly fused. The pterygoids and palatines are highly connected, forming a rigid unit that articulates with the braincase via well-developed basipterygoid processes, while a contact with the parasphenoid is not present (see Bellairs & Jenkin 1960; Zusi 1993; Gussekloo et al. 2001, Mayr 2017; Fig. 1A). In contrast, neognath birds possess a movable joint between pterygoid and palatine, which plays an important role in the kinematic movement of the upper jaw. Here, the pterygoid articulates with the parasphenoid, while the basipterygoid processes are often reduced. The vomer is highly variable in size and shape and often has no connection with the upper jaw beyond an association with the nasal septum and the palatine. In some neognaths, the vomer is greatly

reduced or even absent (see Bellairs & Jenkin 1960; Bock 1964; Zusi 1993; Mayr 2017, Fig. 1A).

In a recent paper, Hu et al. (2019) investigated palate evolution in crown birds and their stem, focusing on the morphology of the vomer. Using 3D geometric morphometrics, the study found that the vomeral shape of neognaths is clearly distinguishable from palaeognaths, in that the latter group has a stronger similarity with their non-avian ancestors. Linking vomer shape with the kinetic abilities of the skull, the authors concluded that cranial kinesis represents an innovation of Neognathae. Furthermore, the authors concluded that vomeral morphology allows for a taxonomic differentiation between the major groups of neognaths, namely Aequorlitornithes, Galloanseres, Gruiformes, and Inopinaves. However, according to their PCA results, all groups strongly overlap each other within PC1, while a taxonomic differentiation is only noticeable within PC2 (other principal components are not shown). Taking the great size variation of the vomer of neognath birds into account (Zusi 1993), we wonder if the reported taxonomic differentiation between palaeognaths and the neognath subclades could alternatively be related to allometry, i.e. the dependence of shape on size (Klingenberg 1998), rather than pure shape variation. In order to test this hypothesis, we re-analysed the dataset of Hu et al. (2019), comparing allometric shape data with non-allometric residuals, and re-evaluating the role of the vomer in the evolution of cranial kinesis in crown birds.

Materials and Methods

The published 3D models and landmarks data of 41 specimens including 36 species were downloaded from Hu et al. 2019 (https://doi.org/10.6084/m9.figshare.7769279.v2). This dataset contains five extinct species (two stem line representatives: the troodontid *Sinovenator changii*, the Avialae *Sapeornis chaoyangensis*; and three fossil palaeognath

crown birds from the clade Dinornithiformes: *Pachyornis australis*, *Megalapteryx didinus* and *Diornis robustus*), five extant Paleognathae and 27 extant Neognathae representing the two major clades of crown birds.

The original landmarks data (Dataset A) is composed of five anatomical landmarks and 43 semi-landmarks (see Hu et al. 2019). The landmark data were imported into the software *R v.3.5.2* (R Core Team, 2018). Using the *plotAllSpecimens* function of *Geomorph v.3.2.1* (Adams *et al*. 2013) in *R*, we notice great variability for each anatomical landmark, resulting from two main shapes in the vomer. First, the majority of bird possesses a fused vomer that is bilaterally symmetric and roof-shaped in transection, having a horizontal orientation within the pterygoid-palatine complex (Fig. 1B). And second, some members of Aequorlitornithes (e.g., *Podiceps nigricollis*, and *Podilymbus podiceps*), Galloanseres (e.g., *Anas crecca*, *Anseranas semipalmata*, and *Cairina moschata*) and Inopinaves (e.g., *Aquila audax*, *Falco cenchroides*, and *Haliastur sphenurus*) have a fused vomer that is completely mediolaterally flattened in transection and vertically orientated within the pterygoid-palatine complex (Fig. 1B). Therefore, we created a second dataset (Dataset B), where species with flat vomer morphology were excluded. Furthermore, the palaeognath birds *Struthio camelus* and *Dromaius novaehollandiae* of the original Dataset A were represented by both juvenile and adult specimens. Because ontogenetic variation could, however, potentially impair size and position of the palaeognath morphospace, we removed the juvenile and subadult specimens of *S. camelus* and *D. novaehollandiae* in order to rerun the analysis just with adult semaphoronts (Dataset C). Finally, we created a fourth dataset, where both juvenile/subadult specimens and species with flat vomers were removed from the sample (Dataset D).

For superposition of the 3D landmark data, we followed Hu et al. (2019) by performing a Generalized Procrustes analysis (*GPA*). The *GPA* was done with the help of the *gpagen* function in *Geomorph*. Afterward, we performed a principal component analysis

(*PCA*) in order to visualize the shape variability of the vomer and the variance of morphospace for two groupings: (1) Paleognathae versus Neoganthae and (2) Paleognathae, Inopinaves, Galloanserae, Gruiformes and Aequorlitornithes. This was done with the *plotTangentSpace* function from *Geomorph*.

Because the vomer showed great variation in centroid size after superimposition, ranging from 14.60 (*Manorina melanocephala*) to 168.318 (*Dromaieus novehollandia*), we tested if there is a significant correlation between Procrustes coordinates and log-transformed centroid size (Goodall 1991) using the function *procD.lm* in *Geomorph*. This function performs a multivariate regression between the shape and size with a permutation of 10,000 iterations. A significant relationship between both parameters indicates that the superimposed shape still contains an allometric signal. Based on this correlation we estimated non-allometric residuals of the Procrustes coordinates and repeated the *PCA*. In addition, we tested each of the first eleven PCs that together describe more than 95 of total variation for allometric signals.

To test for potential overlap in morphospace of vomer shapes in different clades of crown bird (see grouping 1 and 2) and their relation to the stem line representatives *S. changii* and *S. chaoyangensis*, we applied three different multivariate statistical methods, using the first eleven PCs as input data. We first applied a nonparametric multivariate analysis of variance (*perMANOVA*). This method evaluates the potential overlapping of groups in morphospace by testing the significance of their distribution on the basis of permutation (10,000 replications) and Euclidean distance (as one of several possible distance measures), not requiring normal distribution of the data (Anderson, 2001; Hammer & Harper, 2006). The spatial relationship of groups relative to each other is expressed by an F value and p value. For the five-group comparison, the p values were Bonferroni-corrected by multiplying the value with the number of comparisons. Next, we ran a discriminant analysis (*DA*), which

126 reduces a multivariate data set to a few dimensions by maximizing the separation between
127 two or more groups using Mahalanobis distances. This distance measure is estimated from
128 the pooled within-group covariance matrix, resulting in a linear discriminant classifier and an
129 estimated group assignment for each species. The results were cross-validated using
130 Jackknife resampling (Hammer & Harper, 2006; Hammer 2020). Both multivariate tests were
131 done with the program *PAST v.4.03* (Hammer et al. 2001). Finally, we performed a
132 phylogenetic flexible discriminant analysis (*pFDA*) (Schmitz & Motani, 2011; Motani &
133 Schmitz, 2011) in *R*. This method removes the phylogenetic bias from the categorical
134 variables before the actual discriminant analysis is unertaken by estimating Pagel's lambda,
135 which tests how the grouping correlates with phylogeny. This was done for all allometric and
136 non-allometric datasets.

137 For phylogeny, a set of 1,000 relaxed-clock molecular trees, which follow the
138 topology of Hackett et al. (2008) and summarize the range of uncertainties in terms of time
139 calibration of ancestral nodes, were downloaded from birdtree (http://birdtree.org) (Jetz et al.
140 2012, 2014) including all extant bird species in the dataset (Supplementary Data S1). Due to
141 uncertainties in the taxonomic identification of *Aquila sp*., this specimen was removed from
142 the sample as we could not include it in the phylogeny. Because the specimen occupies
143 almost the same position as *Aquilla audax*, we consider this deletion to have a negligible
144 effect on the outcome of the analyses. Furthermore, the species *Sterna bergii* and *Grus*
145 *rubincunda* used in the analysis from Hu et al. (2019) are junior synonyms of *Thalasseus*
146 *bergii* (Bridge et al. 2005) and *Antigone rubicunda* (Krajewski et al. 2010). Using the
147 function *consensus.edges* in the *R* package *phytools v.0.7-20*, we computed a temporal
148 consensus. The extinct dinornithiform species were placed as sister-group to Tinamidae
149 following Mitchell et al. (2014). Because of their recent extinction (Holdaway & Jacomb
150 2000; Turvey & Holdaway 2005), the age was set to zero, similar to the other crown birds.

The stem line representatives *S. changii* and *S. chaoyangensis* were added following the time-calibrated phylogeny of Rauhut et al. (2019). Because of the presence of juvenile specimens in dataset A and B, we added the juvenile specimens by splitting OTU of *S. camelus* and *D. novehollandia* into a polytomy with each OUT having a branch length of one year (this value had to be standardized, as *pFDA* requires an isometric tree).

The error of correct identification from the resulting confusion matrices was compared between allometric and non-allometric data. For these comparisons, we used non-parametric *Mann-Whitney U* and *Kruskal-Wallis* tests, which both estimates, whether or not two univariate samples were taken from populations with equal medians, being more robust against small sample sizes and data without normal distribution (Hammer & Harper 2006). Both tests were run with *PAST*.

Finally, we applied for 19 species an ordinary least square regression analysis to test the correlation between log-transformed vomer and the skull size using a log-transformed box volume (Height x Width x Length). The measurements of the skull box volume were taken from skullsite (https://skullsite.com).

Results

Based on the *PCA* of the original dataset, the first two PCs explain over 52% (Fig. 2A) of total shape variation (PC1: 27.5%; PC2:25.1%). The morphospace of palaeognaths and neognaths is almost equal in size. Taking the small sample size of palaeognaths into account, the size of their morphospace indicates great shape variation. Both groups show a strong overlap along PC1 and a partial overlap along PC2. When comparing neognath subclades, aequorlitornithines show strong overlap along both PCs with the palaeognath morphospace. Gruiforms lie in the overlapping area of both groups. The morphospace of inopinaves and

175 galloanserinae overlap with each other in both axes, but are separated from palaeognaths,
176 aequorlitornithines and gruiforms along PC2.

177 Allometry summarizes about 6.4% of total shape variation. Using non-allometric
178 residuals PC1 explains 29.3% and PC2 22.9% (Fig 2.B). While the general distribution of the
179 single bird clades does not change along PC1, the groups are less separated along PC2, which
180 contains the major allometric signal within the principal components (slope: -0.523; R^2:
181 0.185; p: 0.005; predicted variation: 19.5%), which is 4.9% of total shape variation in the
182 original dataset. Here, the palaeognath morphospace overlaps fully with aequorlitornithines
183 and gruiforms, partly with inopinaves and marginally with galloanserinae. For the three other
184 datasets, we observe more or less similar general trends before and after size correction,
185 although the single morphospaces are partly shrunk. In all cases, the two stem line
186 representatives *Sinovenator changii* and *Sapeornis chaoyangensis* lie within the marginal
187 area of the palaeognaths/aequorlitornithines morphospace. Here, vomer morphology of the
188 troodontid *S. changii* is more bird-like than that of the avialian *S. chaoyangensis*
189 (Supplementary Data S2-S3).

190 In all studied datasets, the *perMANOVA* found a significant separation between
191 palaeognath and neognath birds, showing no impact of allometry. For the five-group
192 comparison of the original dataset (A), the overall results still indicate significant separation
193 between clades for both allometric and non-allometric data. However, group-by-group
194 comparison of allometric data indicates an overlap in morphospace of gruiformes with
195 aequorlitornithines, inopinaves, galloanserinae and palaeognaths. These overlaps of
196 gruiforms with other bird clades persist when allometry is removed from shape, but in
197 addition, aequorlitornithines cannot be distinguished from palaeognaths anymore, as
198 indicated by the *PCA* results (Fig. 2 A,B). The overlap between clades increases with the
199 exclusion of species with flat vomers and non-adult semaphoronts.

For the original dataset (A) with allometry included, the *DA* identifies all species correctly as palaeognaths or neognaths. The error of false identification increases to 2.6% if the data are jack-knifed. When allometry is removed, the error increases to 13.2% before and 36.8% after jack-knife resampling. In the former case, the misidentifications are restricted to neognath birds, which are wrongly classified as palaeognaths, while jack-knifing leads to identification errors in both groups. For the five-group comparison, all species of dataset (A) are correctly identified, when allometry is still present. The error is 18.4% after jack-knife resampling, showing minor mismatches in all clades. Excluding allometry, the error increases to 10.5% before and 47.4% after jack-knifing. While in the former case, a few aequorlitornithine (2) and inopinave (1) species are wrongly identified as palaeognaths (Fig. 2 C,D), palaeognaths cannot be separated from the neognath subclades anymore after resampling. The exclusion of species with flat vomers and non-adult semaphoronts leads to an increase of error.

The *pFDA* found 15.8% of wrong identifications when palaeognaths are compared with neognaths in the original dataset (A). This error increases to 31.6% if shape is corrected for allometry. In both cases, error is primarily based on the wrong identification of palaeognath specimens as neognaths. When palaeognaths are compared with neognath subclades, the error of correct identification is 10.5% before and 26.3% after allometry is removed from the data. For the allometric data, the misidentification result from the overlap between paleognaths, aequorlitornithines and gruiforms. The misidentifications between these three groups are increased when shape is corrected for allometry, while inopinaves are in part also wrongly identified as palaeognaths. The exclusion of species with a flat vomer and/or non-adult semaphoronts usually causes a decrease of false identifications. However, the non-allometric dataset shows an increase in error for the two-group comparison, when species with flat vomers are excluded, and for the five-group comparison, when only adult

225 semaphoronts are taken into account (Fig. 2 E,F). Nevertheless, for all four datasets, the error
226 of correct identification is significantly higher for non-allometric vomer shapes (Fig 3A,
227 Supplementary Data S4).
228
229 **Discussion**
230 The skull of crown birds possesses a complex kinetic system that includes a mobilized
231 quadrate, the zygomatic arch (= jugal bar) and the pterygoid-palatine complex (PPC) that
232 allows for the simultaneous, but restricted motion of both jaws (Bock 1964; Zusi 1984).
233 According to Zusi (1984), the kinetic system can be differentiated into three main types. (1)
234 Prokinesis describes the rotation of the whole beak around the nasal-frontal hinge. (2)
235 Amphikinesis is derived from prokinesis, including the rotation of the beak around the nasal-
236 frontal hinge plus an additional flexion of the anterior portion of the beak. (3) In contrast,
237 rhynchokinesis includes a simple flexion of the beak around one or several bending zones
238 rostral to the nasal-frontal suture, lacking a true hinge. Depending on the position of the
239 bending zones, rhynchokinesis can be further differentiated into five subtypes. Most
240 palaeognath birds possess central rhynchokinesis, while neognaths have realized all types of
241 cranial kinesis (Zusi 1984), including some taxa with akinetic skulls (Reid 1835; Sims 1955;
242 Degrange et al. 2010). In the past, several authors (Hofer 1954; Simonetta 1960; Bock 1963)
243 suggested a close relationship between the morphology of the PPC and type of cranial
244 kinesis. However, Gussekloo et al. (2001) demonstrated that all types of kinesis present in
245 crown birds have similar movements of the quadrate, zygomatic arch and PPC. Palaeognaths
246 and neognaths only differ in the magnitude of kinetic movements in that palaeognaths have
247 slightly more restricted movement due to their rigid palate missing a movable joint between
248 the pterygoid and palatine (Gussekloo et al. 2005).

Thus, although the geometric morphometric results of the vomer shape by Hu et al. (2019) implicate at first view a distinct separation between palaeognaths and neognaths, this separation does not necessarily reflect their conclusions regarding the evolution of cranial kinesis in crown birds. As indicated by the *PCA*, palaeognaths occupy an enormous vomeral morphospace (Hu et al. 2019), which mirrors their generally large palatal disparity (see McDowell 1948) and partly overlaps with gruiforms and aequorlitornithines. In all cases tested, however, the exclusion of allometric shape variation generally increases the error of misidentification between all groups, indicating that the taxonomic distinctions of shape found by Hu et al. (2019) are at least partly an artefact of size. This primarily concerns PC2, which according to Hu et al. (2019) separates palaeognaths from neognaths, but also contains the major allometric information. According to shape variation explained by PC2, larger birds tend to evolve vomers that are more dorsoventrally compressed. Only members of the galloanserinae could be still identified with a high amount of certainty when allometry is excluded.

Thus, our finding supports previous studies that demonstrated a relevant impact of allometry on skull shape evolution in birds (Klingenberg & Marugán-Lobón 2013; Bright et al. 2016; Linde-Medina 2016; Tokita et al. 2016, Bright et al. 2019). By modifying the dataset, it becomes further clear that both the homoplastic presence of flat vomers in aequorlitornithines, inopinaves, galloanserinae (Dataset B) and ontogenetic variation (Dataset C) affects the accuracy of taxonomic identification. In addition, palaeognaths and neognaths do not differ in vomer size when compared to the head size (Fig. 3B). Consequently, vomer shape is not practical for taxonomic identification and should not be used as a proxy to infer the presence or absence of cranial kinesis in crown birds or their stem. In fact, *DA* and *pFDA* frequently identified the troodontid *Sinovenator changii* and avialan *Sapeornis chaoyangensis* as neognaths or neognath subclades when allometry is excluded, while the

original dataset implied a referral to palaeognaths (see also Hu et al. 2019). However, the skull anatomy of both species indicates no cranial kinesis (Xu et al. 2002; Wang et al. 2017; Yin et al. 2018; Hu et al. 2020).

The origin and evolution of cranial kinesis in the stem line of birds is still not well understood due to the rarity of complete three-dimensional skulls. However, skull material from the ornithurines *Ichthyornis dispars* and *Hesperornis regalis* indicates a certain degree of rhynchokinesis (Bühler et al. 1988; Field et al. 2018) that might be comparable to that of extant palaeognaths or some aequorlitornithines, but further shows that this functional character was already present before the origin of the crown. Their kinesis is indicated by the loss of the jugal-postorbital bar and the ectopterygoid (resulting in a loss of contact in the jugal with the skull roof and the palate), the presence of a mobile bicondylar quadrate and a mobile joint between quadrate and quadratojugal. Recently, Plateau & Foth (2020) speculated that the peramorphic bone fusion in the braincase could be also related to cranial kinesis, in which the fusion-induced immobility constrains a controlled kinetic dorsoventral flexion of the avian beak during biting/picking. Based on these characters, most Mesozoic Avialae (including *Sapeornis chaoyangensis*) still had akinetic skulls, although some Enantiornithes possessing a reduced jugal-postorbital bar might have evolved primitive kinesis convergently to Ornithurae (O'Connor & Chiappe 2011).

Acknowledgements

We thank Walter Joyce for comments on the manuscript and the Swiss National Science Foundation (PZ00P2_174040 to C.F.) for financial support.

Additional information

Funding

This study was funded by the Swiss National Science Foundation (PZ00P2_174040).

Competing interests

The authors declare no competing interests.

Author Approvals

All authors have seen and approved the manuscript. The manuscript has not been accepted or published elsewhere.

Author contributions

O.P. and C.F. designed the research project and analysed the data; and O.P. and C.F. wrote the paper and prepared all figures.

Data availability

The 3D models and landmarks data of Hu et al. (2019) are available at Figshare (DOI: https://doi.org/10.6084/m9.figshare.7769279.v2).

Supplementary information

- Data S1: Phylogenetic trees used for *pFDA.*
- Data S2: PCA results of all dataset before and after correction for allometry.
- Data S3: PCA plots of Dataset B-D before and after correction for allometry.
- Data S4: Results of npMANOVA, DA and pFDA.
- Data S5: R Code including all statistical analyses.

References

Adams DC, Otárola-Castillo E. 2013. *geomorph*: an *R* package for the collection and analysis of geometricmorphometric shape data. *Methods in Ecology and Evolution* 4:393–399.

Anderson MJ. 2001. A new method for non-parametric multivariate analysis of variance. *Austral Ecology* 26:32–46.

Bellairs ADA, Jenkin CR. 1960. The skeleton of birds. In: Marshall AJ ed. *Biology and Comparative Physiology of Birds, Vol. 1*. New York: Academic Press, 241–300.

Bock WJ. 1963. The cranial evidence for ratite affinities. *Proceedings of the 13th International Ornithological Congress* 1:39–54.

Bock WJ. 1964. Kinetics of the avian skull. *Journal of Morphology* 114:1–42.

Bridge ES, Jones AW, Baker AJ. 2005. A phylogenetic framework for the terns (Sternini) inferred from mtDNA sequences: implications for taxonomy and plumage evolution. *Molecular Phylogenetics and Evolution* 35:459–469.

Bright JA, Marugán-Lobón J, Cobb SN, Rayfield J. 2016. The shapes of bird beaks are highly controlled by nondietary factors. *Proceedings of the National Academy of Sciences, U.S.A.* 113:5352–5357.

Bright JA, Marugán-Lobón J, Rayfield J, Cobb SN. 2019. The multifactorial nature of beak and skull shape evolution in parrots and cockatoos (Psittaciformes). *BMC Evolutionary Biology* 19:1–9.

Bühler P, Martin LD, Witmer LM. 1988. Cranial kinesis in the Late Cretaceous birds *Hesperornis* and *Parahesperornis*. *The Auk* 105:111–122.

Degrange F, Tambussi C, Moreno K, Witmer L, Wroe S. 2010. Mechanical analysis of feeding behavior in the extinct "Terror Bird" *Andalgalornis steulleti* (Gruiformes: Phorusrhacidae). *PLoS ONE* 5:e11856.

Field DJ, Hanson M, Burnham DA, Wilson LE, Super K, Ehret D, Ebersole JA, Bhullar B-AS. 2018. Complete *Ichthyornis* skull illuminates mosaic assembly of the avian head.

Nature 557:96–100.

Goodall C. 1991. Prorustes methods in the statistical analysis of shape. *Journal of the Royal Statistical Society: Series B (Methodological)* 53:285–321.

Gussekloo SWS, Bout RG. 2005. The kinematics of feeding and drinking in palaeognathous birds in relation to cranial morphology. *The Journal of Experimental Biology* 208:3395–3407.

Gussekloo SWS, Vosselman MG, Bout RG. 2001. Three-dimensional kinematics of skeletal elements in avian prokinetic and rhynchokinetic skull determined by roentgen stereophotogrammetrics. *The Journal of Experimental Biology* 204:1735–1744.

Hackett SJ, Kimball RT, Reddy S, Browie RCK, Braun EL, Chojnowski JL, Cox A, Han K, Harshman J, Huddleston CJ, Marks BD, Miglia KJ, Moore WS, Sheldon FH, Steadman DW, Witt CC, Yuri T. 2008. A phylogenomic study of birds reveals their evolutionary history. *Science* 320:1763–1768.

Hammer O, Harper DAT. 2006. *Paleontological Data Analysis*. Malden: Blackwell Publishing.

Hammer O, Harper DAT, Ryan PD. 2001. PAST: paleontological statistics software package for education and data analysis. *Palaeontologia Electronica* 4:1–9.

Hammer O. 2020. *PAST Paleontological Statistics v.4.03. Reference Manual.* Oslo: University of Oslo.

Hofer H. 1954. Neuere Untersuchungen zur Kopfmorphologie der Vögel. *Acta XI Congressus Internationalis Ornithologici*:104–137.

Holdaway RN, Jacomb C. 2000. Rapid extinction of the moas (Aves: Dinornithiformes): model, test, and implications. *Science* 287:2250–2254.

Hu H, O'Connor J, McDonald P, Wroe S. 2020. Cranial osteology of the Early Cretaceous *Sapeornis chaoyangensis* (Aves: Pygostylia). *Cretaceous Research* 113:104496.

374 Hu H, Sansalone G, Wroe S, McDonald PG, O'Connor JK, Li Z, Xu X, Zhou Z. 2019.
375 Evolution of the vomer and its implications for cranial kinesis in Paraves. *Proceedings*
376 *of the National Academy of Sciences, U.S.A.* 116:19571–19578.
377 Huxley TH. 1867. On the classification of birds; and on the taxonomic value of the
378 modifications of certain cranial bones observable in the class. *Proceedings of the*
379 *Zoological Society of London* 27:415–472.
380 Jetz W, Thomas GH, Joy JB, Hartmann K, Mooers AO. 2012. The global diversity of birds in
381 space and time. *Nature* 491:444–448.
382 Jetz W, Thomas GH, Joy JB, Redding DW, Hartmann K, Mooers AO. 2014. Global
383 distribution and conservation of evolutionary distinctness in birds. *Current Biology*
384 24:1–12.
385 Klingenberg CP. 1998. Heterochrony and allometry: the analysis of evolutionary change in
386 ontogeny. *Biological Reviews* 73:79–123.
387 Klingenberg CP, Marugán-Lobón J. 2013. Evolutionary covariation in geometric
388 morphometric data: analyzing integration, modularity, and allometry in phylogenetic
389 context. *Systematic Biology* 62:591–610.
390 Krajewski C, Sipiorski JT, Anderson FE. 2010. Complete mitochondrial genome sequences
391 and the phylogeny of cranes (Gruiformes: Gruidae). *The Auk* 127:440–452.
392 Linde-Medina M. 2016. Testing the cranial evolutionary allometric "rule" in Galliformes.
393 *Journal of Evolutionary Biology* 29:1873–1878.
394 Mayr G. 2017. *Avian evolution*. Chichester: John Wiley.
395 McDowell S. 1948. The bony palate of birds. Part I. The Palaeognathae. *The Auk* 65:520–
396 549.
397 Mitchell K, Llamas B, Soubrier J, Rawlence N, Worthy T, Wood J, Lee M, Cooper A. 2014.
398 Ancient DNA reveals elephant birds and kiwi are sister taxa and clarifies ratite bird

399 evolution. *Science* 344:898–900.

400 Motani R, Schmitz L. 2011. Phylogenetic versus functional signals in the evolution of form-
401 function relationships in terrestrial vision. *Evolution* 65:2245–2257.

402 O'Connor JK, Chiappe LM. 2011. A revision of enantiornithine (Aves: Ornithothoraces)
403 skull morphology. *Journal of Systematic Palaeontology* 9:135–157.

404 Plateau O, Foth C. 2020. Birds have peramorphic skulls, too: anatomical network analyses
405 reveal oppositional heterochronies in avian skull evolution. *Communications Biology* 3.

406 R Development Core Team. 2011. *R*: a language and environment for statistical computing.
407 *http://www.r-project.org*.

408 Rauhut OWM, Tischlinger H, Foth C. 2019. A non-archaeopterygid avialan theropod from
409 the Late Jurassic of southern Germany. *eLife* 8:e43789.

410 Reid J. 1835. Anatomical description of the Patagonian penguin. *Proceedings of the*
411 *Zoological Society of London* 3:132–148.

412 Revell LJ. 2012. *phytools*: an *R* package for phylogenetic comparative biology (and other
413 things). *Methods in Ecology and Evolution* 3:217–223.

414 Schmitz L, Motani R. 2011. Nocturnality in dinosaurs inferred from scleral ring and orbit
415 morphology. *Science* 332:705–708.

416 Simonetta A. 1960. On the mechanical implications of the avian skull and their bearing on
417 the evolution and classification of birds. *The Quaterly Review of Biology* 35:206–220.

418 Sims S. 1955. The morphology of the head of the hawfinch (*Coccothraustes coccothraustes*).
419 *Bulletin of the British Museum* 2:371–393.

420 Tokita M, Yano W, James H, Abzhanov A. 2016. Cranial shape evolution in adaptive
421 radiations of birds: comparative morphometrics of Darwin's finches and Hawaiian
422 honeycreepers. *Philosophical Transactions of the Royal Society B* 372:20150481.

423 Turvey ST, Holdaway RN. 2005. Postnatal ontogeny, population structure, and extinction of

the giant moa *Dinornis*. *Journal of Morphology* 265:70–86.

Wang Y, Hu H, O'Connor JK, Wang M, Xu X, Zhou Z, Wang X, Zheng X. 2017. A previously undescribed specimen reveals new information on the dentition of *Sapeornis chaoyangensis*. *Cretaceous Research* 74:1–10

Xu X, Norell MA, Wang X, Makovicky PJ, Wu X. 2002. A basal troodontid from the Early Cretaceous of China. *Nature* 415:780–784.

Yin Y, Pei R, Zhou C. 2018. Cranial morphology of *Sinovenator changii* (Theropoda: Troodontidae) on the new material from the Yixian Formation of western Liaoning, China. *PeerJ* 6:e4977. DOI: 10.7717/peerj.4977.

Zusi RL. 1984. A functional and evolutionary analysis of rhynchokinesis in birds. *Smithsonian Contributions to Zoology* 395:1-40.

Zusi RL. 1993. Patterns of diversity in the avian skull. In: Hanken J, Hall BK eds. *The skull. Vol. 2. Patterns of structural and systematic diversity*. Chicago: University of Chicago Press, 391–437.

Figure legends

Fig. 1. Anatomical organization of the pterygoid-palatine complex (PPC) and shape variability of the vomer in palaeognath and neognath birds. (A) Palates of *Dromaius novaehollandia* (left), *Cygnus olor* (middle) and *Corvus corax* (right) in ventral view (all specimens form the Natural History Museum of Fribourg/University of Fribourg). **(B)** 3D models of the vomer of *Dinornis robustus*, *Anas crecca* and *Corvus sp.* in lateral view (left) and anterior view (right) from (not at scale) (3D models from Hu et al. 2019). Max, Maxillary; Pal, Palatine; Premax, Premaxilary; Pter, Pterygoid; Vom, Vomer.

448 **Fig. 2. Differences between allometric and non-allometric morphospaces of the vomer**
449 **(Dataset A) in palaeognath and neognath birds. (A)** *PCA* results of allometric data. **(B)**
450 *PCA* results of non-allometric data. **(C)** *DA* results of allometric data. **(D)** *DA* results of non-
451 allometric data. **(E)** *pFDA* results of allometric data. **(F)** *pFDA* results of non-allometric data.
452
453 **Fig. 3. Errors of correct taxonomic identification for all comparisons of Dataset A-D.**
454 **(A)** Two-group identification (Palaeognathae and Neognathae) before (red) and after (green)
455 correction for allometry. *DA*, Discriminant analysis; *DA*JK*, Discriminant Analysis with
456 jackknife resampling; *pFDA*, phylogenetic Flexible Discriminant Analysis. **(B)** Five-group
457 identification (Palaeognathae, Aequorlitornithes, Galloanserae, Gruiformes and Inopinaves).
458 **(C)** *OLS* regression (black line) between log-transformed skull box volume and log-
459 transformed centroid size of the vomer. Grey shadow mark the area of the 95% confidence
460 interval.

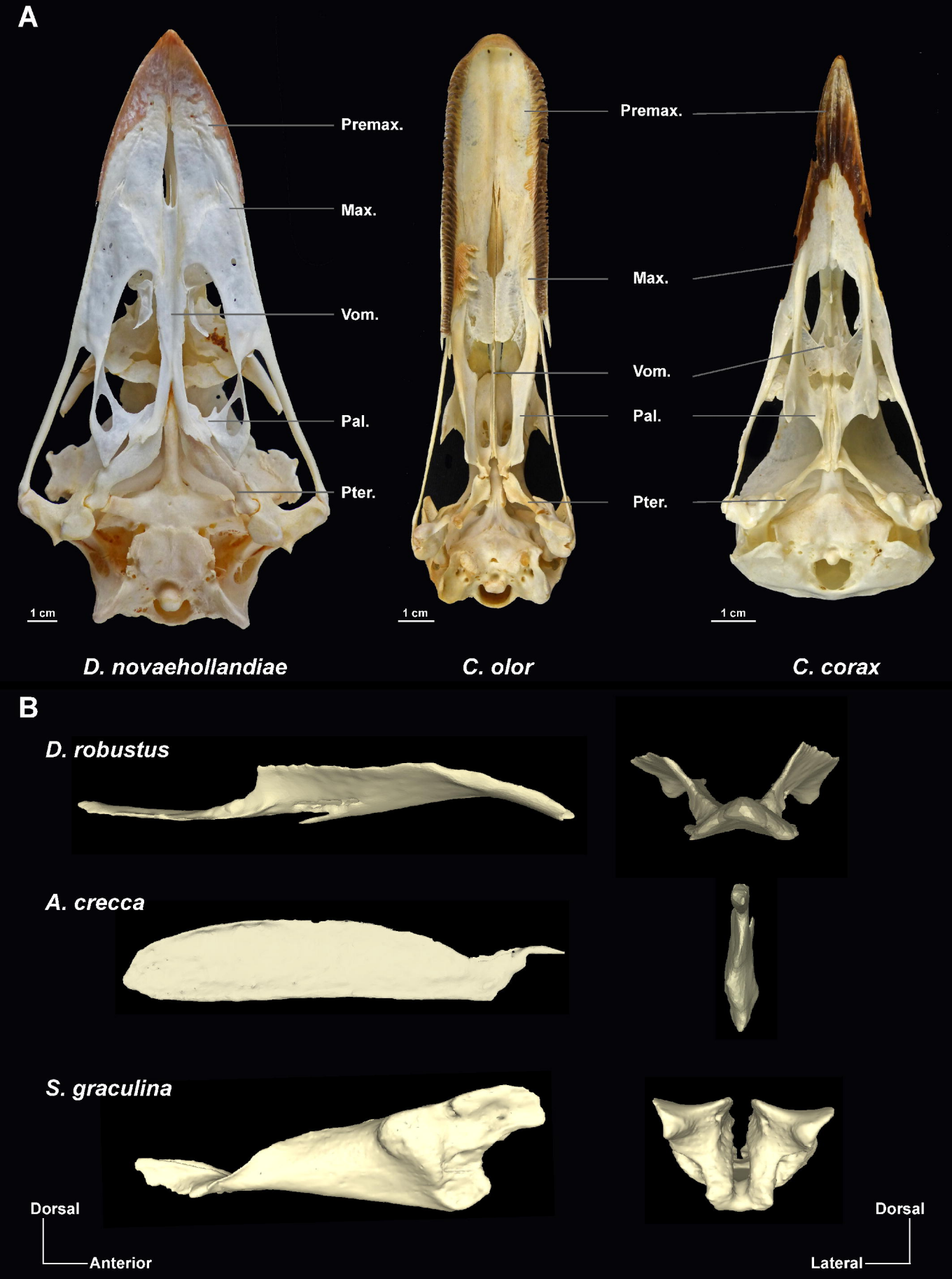
A
Premax.
Max.
Vom.
Pal.
Pter.
1 cm
Premax.
Max.
Vom.
Pal.
Pter.
1 cm
1 cm
D. novaehollandiae
C. olor
C. corax
B
D. robustus
A. crecca
S. graculina
Dorsal
Anterior
Dorsal
Lateral

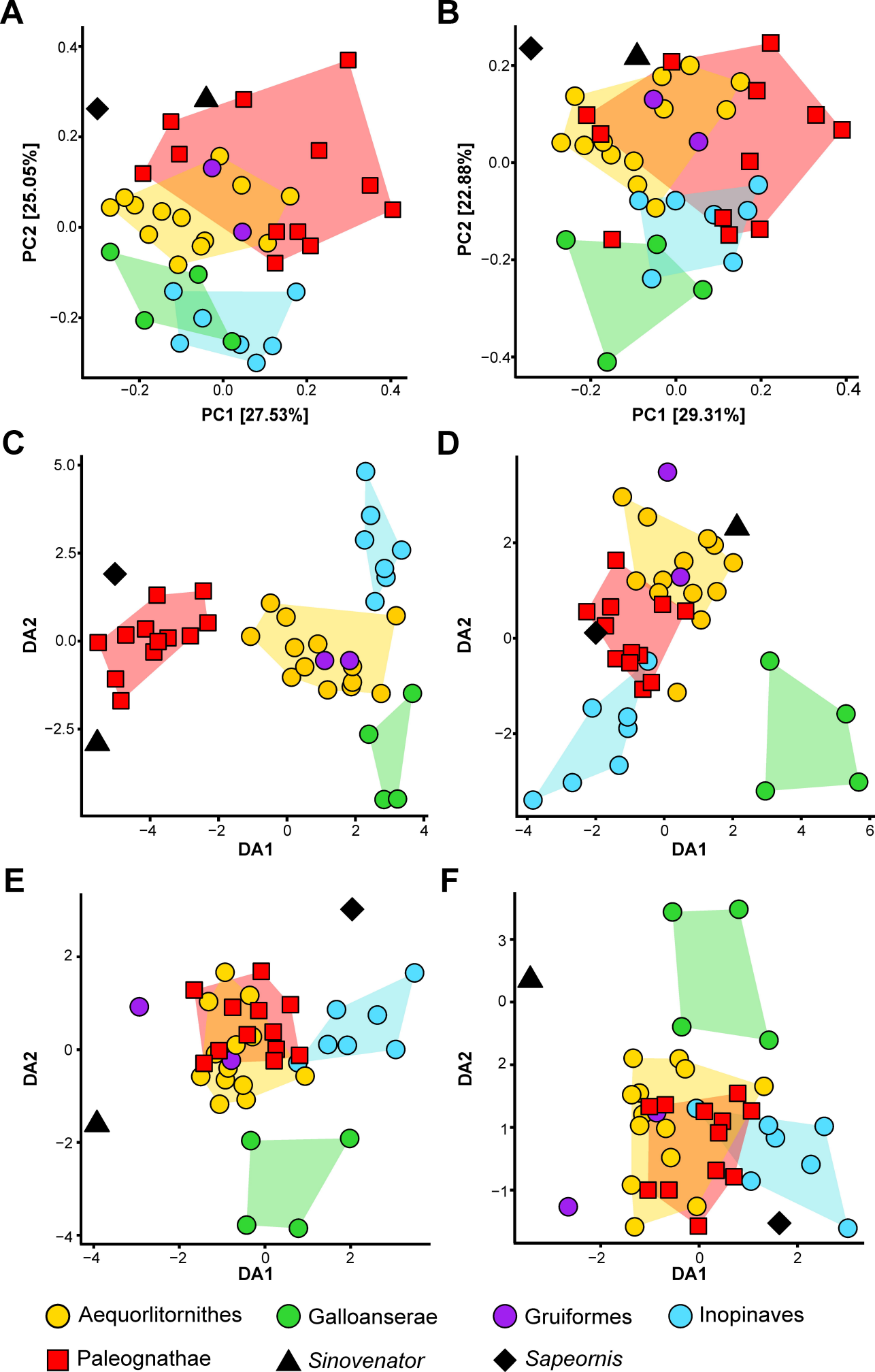
A
B
C
D
E
F
PC1 [27.53%]
PC2 [25.05%]
PC1 [29.31%]
PC2 [22.88%]
DA1
DA2
Aequorlitornithes
Galloanserae
Gruiformes
Inopinaves
Paleognathae
Sinovenator
Sapeornis

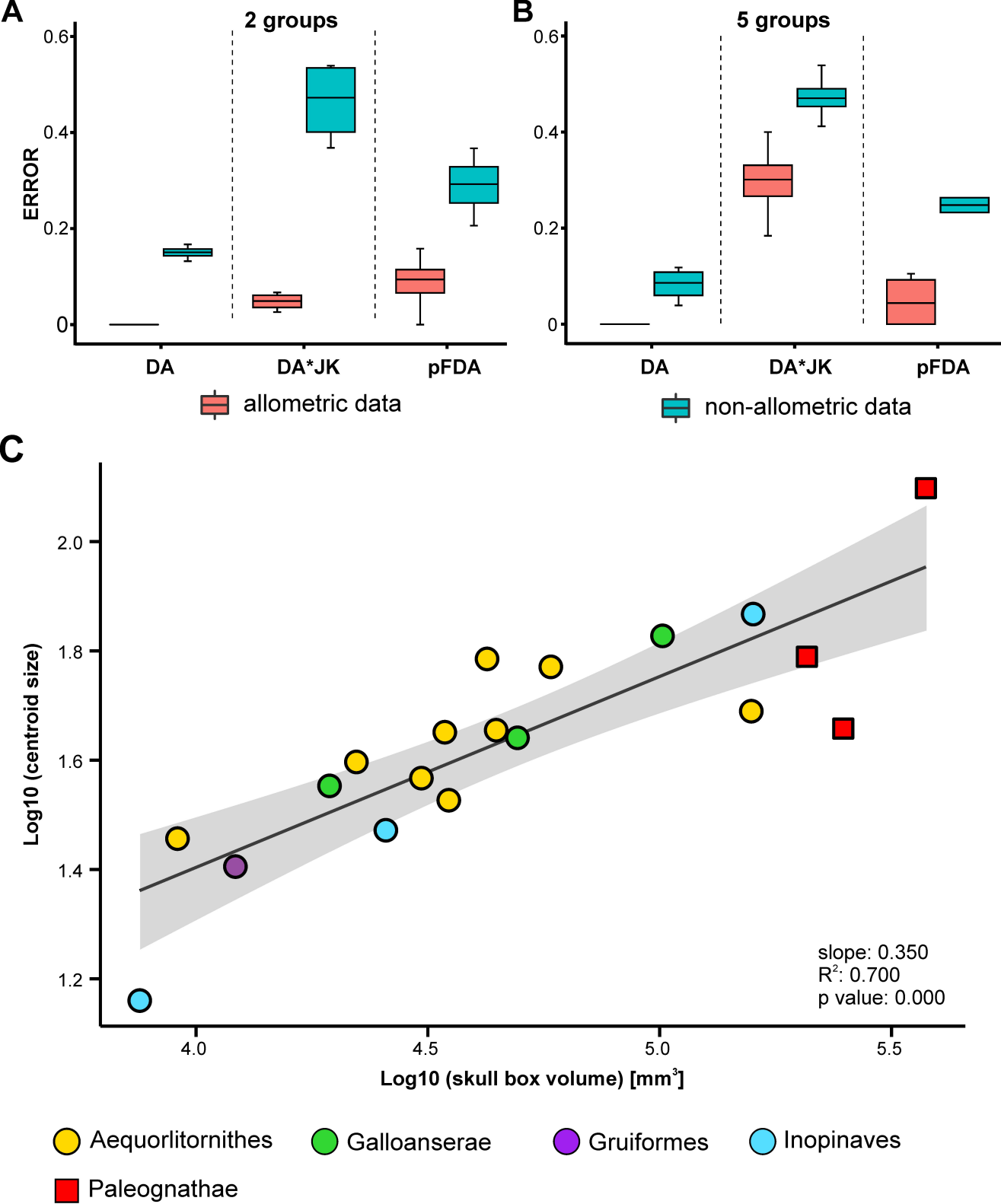
A
2 groups
ERROR
0.6
0.4
0.2
0
DA
DA*JK
pFDA
allometric data
B
5 groups
0.6
0.4
0.2
0
DA
DA*JK
pFDA
non-allometric data
C
Log10 (centroid size)
2.0
1.8
1.6
1.4
1.2
4.0
4.5
5.0
5.5
Log10 (skull box volume) [mm3]
slope: 0.350
R2: 0.700
p value: 0.000
Aequorlitornithes
Galloanserae
Gruiformes
Inopinaves
Paleognathae